Ab initio Calculation of Tunneling Current through Ultra-Thin SiO_2 Gate Dielectrics of MOS Structures, Including the Influence of Oxygen Vacancies on the Tunneling Current

E. Nadimi*, R. Janisch** and C. Radehaus*

*Technical University of Chemnitz, Reichenhainer Str. 70, 09126, Chemnitz, Germany, ebn@hrz.tu-chemnitz.de, cvr@zfm.tu-chemnitz.de
**Friedrich-Alexander-University Erlangen-Nuremberg, Martensstrasse 5, 91058 Erlangen, Germany, rebecca.janisch@ww.uni-erlangen.de

ABSTRACT

Ab initio density functional theory and ballistic transport theory are applied to the calculation of tunneling current through ultra-thin SiO_2 gate dielectrics. The $Si/SiO_2/Si$ model interface has been constructed by orienting a crystalline SiO_2 (β–cristobalite) slab such that the misfit with Si (001) was minimized and no dangling bonds appear at the interface. The structure was then sandwiched between two n^+-doped Si contacts and tunneling current was calculated using ballistic transport theory. Different oxygen vacancies were created in SiO_2 and their influence on the tunneling current was studied. All vacancies result in an increase of tunneling current. However arm vacancies (between a surface Si atom and the first Si layer in bulk SiO_2) seem to have the most destructive effect on tunneling current at low biases. Different bulk vacancies show almost equal influence on the tunneling current.

Keywords: metal-oxide-semiconductor devices, leakage current, ab initio density functional theory, ballistic transport

1 INTRODUCTION

Improving the performance of metal-oxide-semiconductor field effect transistor (MOSFET) devices in terms of a higher degree of integration and faster devices has required a larger gate capacitance for each new technology generation. To date, this has been achieved mainly by decreasing the gate oxide thickness, which has reached values as small as 1.5 *nm*. Further down-scaling of SiO_2 is not possible due to intolerably high gate leakage current. Therefore, integration of new gate dielectric materials with higher permittivity is inevitable in the next MOSFET generation. However, the transition layer between Si and SiO_2 still plays a central role. Indeed, during the post-deposition annealing for dopant activation, oxygen atoms diffuse out of the high-k dielectric and oxidize the Si substrate, forming an interfacial silicon oxide layer.

Calculation of gate tunneling current through such thin and complex gate stacks, as a major design consideration, is of great importance. To date, most calculations of tunneling current through SiO_2 or other stacked gate dielectrics are based on the effective mass approximation; either assuming a single parabolic dispersion with an energy-independent tunneling effective mass [1-4] or a Franz-type energy-dependent one [5-7]. However, in ultra-thin gate dielectrics the effective mass approximation fails [8], and an atomic-scale approach is necessary. On the other hand, it is unclear how to associate an effective mass to a stacked gate dielectric with an interfacial layer and complex profile of transition metals or nitrogen. Furthermore, applying an atomic-scale approach provides a method to investigate atomic scale bonding, dislocations and vacancies, as well as their influence on the tunneling current.

In the following report, a combination of density functional theory (DFT) and ballistic transport theory is applied to the calculation of a $Si/SiO_2/Si$ model interface and the tunneling current through this structure, containing different oxygen vacancies. Applying ballistic transport theory seems to be justified since oscillations in Fowler-Nordheim tunneling currents (a sign of coherency) persist up to thicknesses of 6 *nm* and the mean free path is estimated to be about 1-2 *nm* [9,10].

2 ATOMISTIC STRUCTURAL MODEL

In most electronic structure calculations different phases of crystalline SiO_2 have so far been employed to generate model interfaces, mainly β-quartz [11-13], β-cristobalite [11,14,15] and tridymite [12-14,16]. The electronic structure of these model interfaces has been investigated successfully with the aim of understanding effects such as Si core-level shifts [14], tunneling processes [12], and the carrier mobility in the channel [17]. We started with crystalline SiO_2 β-cristobalite to model the gate oxide. SiO_2 β-cristobalite has a slightly larger lattice mismatch (about 6%) to Si (001) than tridymite, however, cubic cristobalite has a lot of polymorphs that are almost energetically degenerate and differ only by relative rotations of the SiO_4 tetrahedral units.[18] Thus it can adjust easily to stress and to local distortions e.g. due to a vacancy. The mismatch is minimized if the SiO_2 crystal is rotated by 45° around its **c** axis. Thus, the lateral lattice constant of SiO_2 was fixed (expanded) to the value of $\sqrt{2}\times a^{Si}$ and the cristobalite cell was relaxed along its c direction. From the "tetragonal" β-cristobalite bulk structure that was produced by this procedure, a slab consisting of seven layers of SiO_2 was composed and put on the Si substrate consisting of nine

NSTI-Nanotech 2007, www.nsti.org, ISBN 1420061828 Vol. 1, 2007

layers of Si, as shown in Fig. 1. These numbers of atomic layers ensure that bulk properties are recovered in the respective slabs [11,15] and that the interface does not interact with its periodic image. Note that the interface at the right hand side of the supercell is equivalent to the one in the left hand side, but rotated by 90° around the z direction of the supercell (the direction perpendicular to the interface).

To make up for the undercoordination of Si at the interface to SiO_2, extra bridging oxygen atoms were added, completing the coordination. As pointed out in reference [19] by ensuring the preferred coordination number for each Si atom the interface energy is minimized. In this case this also leads to a formal oxidation state +2 of Si at the interface, which is one of the intermediate oxidation states that have been observed experimentally [20]. Different lateral arrangements of the O atoms in the interfacial layer are possible, which would lead to equivalent distributions of oxidation states. However, the details of the distribution do not affect electronic properties of the interface such as the valence band offset [21].

Different initial separations between the last layer of Si in the substrate and the first layer of Si in SiO_2 were chosen. For all the different configurations the atomic positions were relaxed. In the minimum energy configuration the separation between the last layer of Si in Si and the first layer of Si in SiO_2 is 2.32 Å. This means an expansion of almost 73% compared to the lattice spacing along [001] in bulk Si (1.34 Å), and of 32% compared to the separation of the Si planes along [001] in bulk SiO_2 (1.76 Å). However, the Si-O bond lengths at the interface are 1.67 Å from the Si substrate to the oxygen layer, and 1.65 Å from the first layer of Si in SiO_2 to the oxygen layer. This represents only a slight extension of less than 2.5% compared to the Si-O bond length of 1.63 Å in the SiO_2 bulk region.

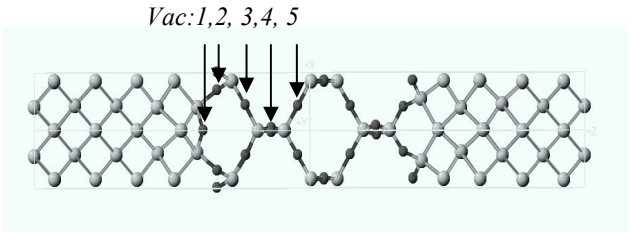

Figure 1: interface structure model of $Si/SiO_2/Si$ system and the positions of five different oxygen (dark balls) vacancies.

3 ELECTRON TRANSPORT THEORY

Tunneling is the dominant leakage current mechanism in ultra-thin oxide layers at low bias and can be evaluated using a simple scattering theory approach. The scattering region (thin dielectric layer) is sandwiched between two semi-infinite degenerate (metallic) Si contacts. Applying the Fermi golden rule, considering all tunneling processes that start from left electrode and end at the right electrode, and taking the state occupancies into account; the current could be expressed as:

$$I=\frac{8\pi^2 e}{h}\sum_{lr}\left|T_{lr}(E)\right|^2\left[f(E-\mu_l)-f(E-\mu_r)\right]\delta(E_l-E_r), \quad (1)$$

where $T_{lr}(E)$ is the matrix element of Lippmann-Schwinger scattering operator $\boldsymbol{T}$ between left and right electrodes, which is accurate to all orders [22]. μ_l and μ_r are the electrochemical potentials of the left and right electrodes, respectively. In the presence of an applied potential, $\mu_l=E_f-\eta eV$ and $\mu_r=E_f+(1-\eta)eV$ with $\eta=0.5$ as suggested by Datta [23]. In the limit of low temperature, where the Fermi distribution takes the step function form, the total current expression reduces to:

$$I=\frac{2e}{h}\int_{\mu_l}^{\mu_r} dE\, T(E), \quad (2)$$

where the transmission function is given by:

$$T(E)=4\pi^2\sum_{lr}\left|T_{lr}(E)\right|^2\delta(E-E_l)\delta(E-E_r). \quad (3)$$

The transmission function can be expressed in terms of Green's functions of the scattering region embedded between two semi-infinite contacts [8].

$$T(E)=Tr[\mathbf{\Gamma}_l\mathbf{G}\mathbf{\Gamma}_r\mathbf{G}^+], \quad (4)$$

where **G** is the Green's function of the scattering region coupled to the left and right electrodes, and the **Γ** operator is the non Hermitian part of the Hamiltonian and describes the level broadening due to coupling of the scattering region with the electrodes [22]. The Green's function operator is given as follows [22]:

$$\mathbf{G}=\frac{\mathbf{I}}{E-\mathbf{H}_d^0-\mathbf{\Sigma}_l-\mathbf{\Sigma}_r}, \quad (5)$$

$\mathbf{H}^0{}_d$ is the hermitian Hamiltonian of the isolated scattering region. The complex operators $\mathbf{\Sigma}_{l,r}$ are the self-energies which represent the coupling of the scattering region with contacts through open boundaries. This formalism is a method to solve the Schrödinger equation with open boundaries, and if the many-body interactions are not explicitly included it is equivalent to the non-equilibrium Green's function formalism [24].

We applied the local density approximation (LDA) within the density functional theory (DFT) and above mentioned ballistic transport formalism as implemented in the Transiesta [25] code, using numerical local orbital basis. Norm-conserving non-local pseudopotentials of the Troullier-Martin type were used for all elements. A single-ζ plus polarization (SZP) basis set, which has been shown to produce reasonable results [24], was used with a cut off

energy of 150 Ry in construction of interface model as well as the calculation of *I-V* characteristics. A 4×4×1 Monhkhorst-Pack *k*-point mesh is employed during the relaxation of interface and vacancies, while a much denser *k*-point sampling of 6400 *k*-points is used in the calculation of current.

4 DEFECTS AND TUNNELING CURRENT

We applied the above formalism to the calculation of tunneling current in the structure depicted in figure 1. The Si electrodes are doped by substituting one Si atom with P. Because of the small number of atoms constituting the electrode, this substitution corresponds to a very high doping concentration and the Fermi energy is pushed into the conduction band. Alternatively, other authors [8] use an intrinsic Si electrode and artificially adjust the Fermi level at the conduction band edge.

The tunneling current has been calculated (figure 2) for oxide without any vacancy as well as oxide with five differently-positioned oxygen vacancies *Vac1-Vac5* (figure 1). Vacancies are built in by removing one oxygen atom and relaxing the atomic coordinate of the supercell.

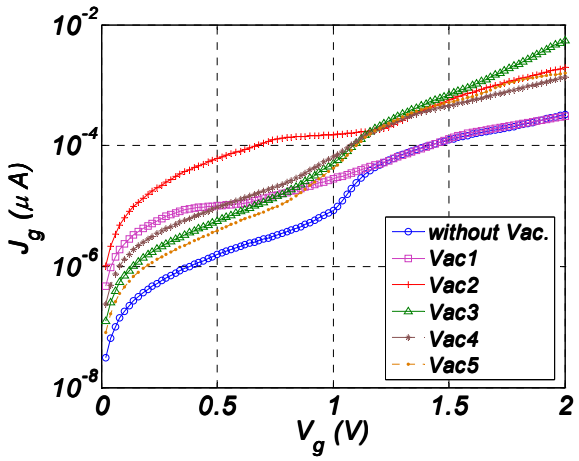

Figure 2: Calculated tunneling current for *Si/SiO$_2$/Si* interface model, without and with vacancies

Vac1 is the so called bridge vacancy and can be considered as a surface defect. Figure 3 shows two peaks in the density of states at the valence band edge of Si as well as around 0.6 *eV* above the Fermi energy, due to Si-Si bond at interface. *Vac2*, the so called arm vacancy, as well as other oxide vacancies (*Vac3-Vac5*) cause a defect state around 0.2 *eV* above the valence band of SiO_2 in agreement with [12]. Figure 4 shows the transmission probability of different samples. The very small transmission probabilities around -1 *eV* represent the *Si* band gap (≈0.51 *eV*), while the small transmission probabilities between -4 and 2 *eV* correspond to the SiO_2 band gap (≈5.85 *eV*).

Figure 2 indicates that the bridge vacancy caused a higher tunneling current at small applied voltages ($V_g \leq 1.2$ *V*) compared to the ideal system. At lower voltages the main contribution to the tunneling current comes from the conduction band electrons of the degenerate Si electrode with energies around the Fermi level. A peak in DOS around 0.6 *eV* above the Fermi energy in *Vac1* provides a high density of empty states and leads to an increase in current. However, increasing the applied voltage above 1.2 *V* shifts this peak under the Fermi level and charges the surface states, causing these states not to participate in carrying the tunneling current. On the other hand, at high energies the transmission probability of the ideal system and *Vac1* become almost equal leading to equal tunneling current at . (V_g>1.2 *V*)

As mentioned above, figure 3 shows that vacancies *Vac2-5* cause the same defect states near the valence band of SiO_2. However, these states could not participate in the tunneling process due to their large distances from the Fermi energy. They cause changes in the potential landscape of the barrier and consequently in the transmission probability of the scattering region. These changes around the Fermi energy are depicted in figure 5. The transmission probability of *Vac2* around the Fermi energy is considerably higher than those of *Vac3-5,* which is the reason for the higher tunneling current of *Vac2* compared to the other samples. The same discussion based on transmission probability is valid for the higher current of *Vac3* around 2 *V*.

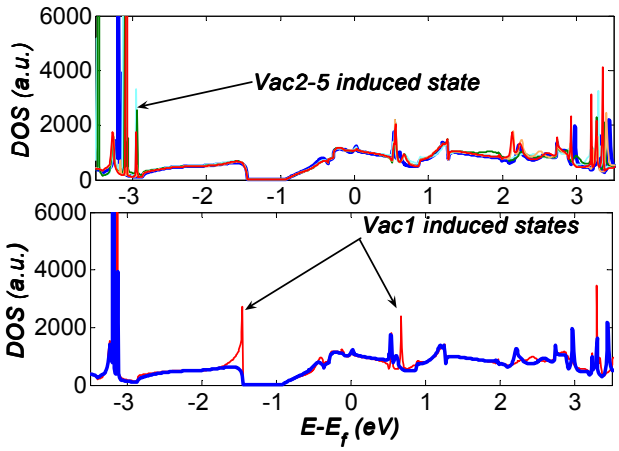

Figure 3: Density of states of the ideal system (thick line-blue) and those containing *Vac2-5* (upper-panel) as well as DOS of the ideal system (thick line-blue) and those containing *Vac1* (lower panel)

In general all different vacancies are shown to cause an enhancement in tunneling current either due to a higher DOS at the conduction band (*Vac1*) or higher transmission probability around the Fermi energy (*Vac2-5*). However the bridge vacancy seems to affect the tunneling process only at low applied biases, and acts like an interfacial state, while the arm vacancy has the most destructive effect on the tunneling current at biases under 1 *V*. Bulk vacancies (*Vac3-5*) show almost the same behavior with small discrepancies at low and high biases.

NSTI-Nanotech 2007, www.nsti.org, ISBN 1420061828 Vol. 1, 2007

5 CONCLUSIONS

A combination of DFT and ballistic transport theory is applied to the construction of a $Si/SiO_2/Si$ interface model structure, as well as the calculation of tunneling current through such a system. Several oxygen vacancies are created at different positions in the model structure and the influence of these vacancies on the tunneling current has been studied. A surface vacancy (*Vac1*) leads to higher tunneling current only at low biases, while bulk oxide vacancies cause an overall enhancement of tunneling current. The arm vacancy produces the highest tunneling current at low biases.

The investigation of two vacancies in the system and their correlation, as well as hole tunneling at the valence band is the subject of prospective research and calculation.

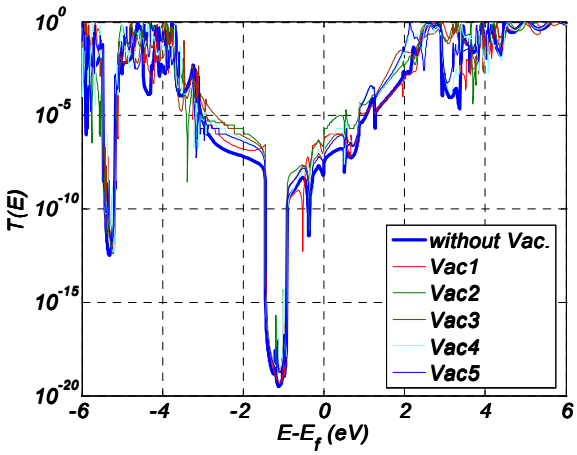

Figure 4: Transmission probability of the ideal system and those containing *Vac1-5*

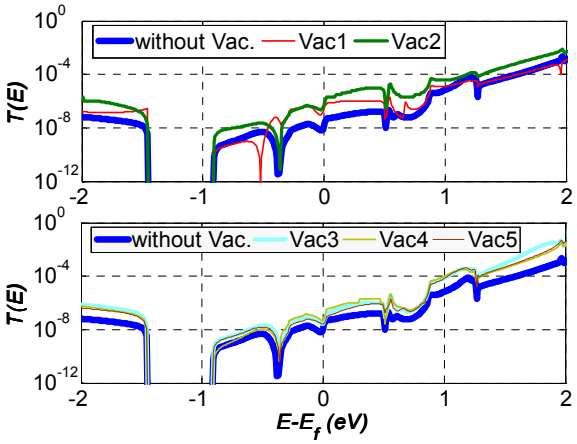

Figure 5: Transmission probability of the ideal system and those containing *Vac1-2* (upper panel); *T(E)* of the ideal system and those containing *Vac3-5* (lower panel)

REFERENCES

[1] M. Fukuda, W. Mizubayashi, A. Kohno, S. Miyazaki and M. Hirose, Jpn, J. Appl. Phys., Part 2 37, L1534, 1998.

[2] E. Cassan, S. Galdin, P. Dollfus and P. Hesto, J. Appl. Phys., 86, 3804, 1999.

[3] S.-H. Lo, D. A. Buchanan, Y. Taur and W. Wang, IEEE Electron Device Lett., 18, 209, 1999.

[4] A. Schenk and G. Heiser, J. Appl. Phys., 81, 7900, 1997.

[5] M. V. Fischetti, S. E. Laux and E. Crabbé, J. Appl. Phys., 78, 1058, 1995.

[6] B. Brar, G. D. Wilk and A. C. Seabaugh, Appl. Phys. Lett., 69, 2728, 1996.

[7] J. Maserjian, J. Vac. Sci. Technol., 11, 996, 1974.

[8] A. A. Demkov, X. Zhang and D. A. Drabold, Phys. Rev. B, 64, 125306-1, 2001.

[9] M. V. Fischetti, D. J. DiMaria, L. Dori, J. Batey, E. Tierney and J. Stasiak, Phys. Rev, B, 35, 4404 1987.

[10] S. Zafar, Q. Liu and E. A. Irene, J. Vac. Sci. Technol. A, 13, 47, 1995.

[11] D. A. Muller, T. Sorsch, S. Moccio, F. Baumann, K. Evans-Lutterodt and G. Timp, Nature, 399, 758, 1999.

[12] M. Städele, B.R. Tuttle and K. Hess, J. Appl. Phys., 89, 348, 2001.

[13] B. R. Tuttle, Phys. Rev. B, 67, 155324, 2003.

[14] A. Pasquarello, M. Hybertsen and R. Car, Phys. Rev. B, 53, 10942, 1996.

[15] S. Tang, R. M. Wallace, A. Seabaugh and D. King-Smith, Appl. Surf. Sci., 135, 137, 1998.

[16] B. R. Tuttle, Phys. Rev. B, 70, 125322, 2004.

[17] X.-Y. Liu, D. Jovanovic and R. Stumpf, Appl. Phys. Lett., 86, 082104, 2005.

[18] Th. Demuth, Y. Jeanvoine, J. Hafner and J.G. Angyan, J.Phys.: Condens. Matter, 11, 3833, 1999.

[19] Yuhai Tu and J. Tersoff, Thin Solid Films, 400, 95, 2001.

[20] F.J. Himpsel, F.R. McFeely, A. Taleb-Ibrahimi, J.A. Yarmoff and G. Hollinger, Phys. Rev. B, 38, 6084, 1988.

[21] F. Giustino, A. Bongiorno and A. Pasquarello, J. Phys. Condens. Matter, 17, S2065 ,2005.

[22] S. Datta, Electronic Transport in Mesoscopic Systems, Cambridge University Press, Cambridge 1995.

[23] Y. Xue and S. Datta, Phys Rev. Lett., 83, 4844, 1999.

[24] L. R. C. Fonseca, A. A. Demkov and A. Knizhnik, Phys. Stat. sol. (b), 239 (1), 48, 2003.

[25] M. Brandbyge, J.-L. Mozos, P. Ordejon, J. Taylor and K. Stokbro, Phys. Rev. B 65, 165401, 2002.